



# Journal of Applied Sciences

ISSN 1812-5654

**science**  
alert

**ANSI***net*  
an open access publisher  
<http://ansinet.com>

## Effect of the Hot Wall Geometry on Laminar Natural Convection in an Inclined Cavity

M. Belkadi, M. Aounallah, A. Azzi, O. Imine and L. Adjout  
 Department of Marine Engineering, Faculty of Mechanics,  
 Applied Mechanics Laboratory (LMA), USTO, Oran, Algeria

**Abstract:** In the present investigation, a numerical study of the effect of the hot wall geometry on a laminar natural convection in an inclined square cavity, differentially heated, was undertaken. This problem is solved by using the partial differential equations which are the equation of mass, momentum and energy. The tests were performed for different inclination angles and Rayleigh numbers while the prandtl number was kept constant. Three geometrical configurations were considered. The results obtained show that the hot wall geometry affects the flow and the heat transfer rate in the cavity. The mean nusselt number decreases compared with the heat transfer in the square cavity.

**Key words:** Natural convection, inclined cavity, undulated hot wall

### INTRODUCTION

Many works relative to numerical and experimental investigations of the natural convection in cavities have been undertaken in the last two decades. In the numerical domain, a big progress has been made<sup>[1-4]</sup> on the natural convection in complex geometries; the study of the heat transfer in a triangular enclosure has been carried out by Hassan<sup>[5]</sup>. He has given some correlations in terms of the nusselt number for different configurations. The natural convection in elliptic cross section has been tested with a single horizontal elliptic cylinder<sup>[6]</sup>. An example of experimental and numerical investigation of the natural convection in the annuli between horizontal confocal elliptic cylinders is performed<sup>[7]</sup>. The physical properties of the fluid which are thermal conductivity, viscosity and the heat capacity were varied<sup>[8]</sup>. The study of the influence of the aspect ratio and inclination angle has been investigated<sup>[9]</sup>.

The natural convection along a vertical wavy surface has been studied theoretically for the application of a cooling fin<sup>[10]</sup>. The results show that the mean nusselt number for a wavy surface is constantly smaller than that of the corresponding flat plate. Indeed, in the renewable energy, some effort has been made in order to reduce the natural convection in the solar collector. Adjout *et al.*<sup>[11]</sup> have studied numerically the influence of the wavy hot wall in an inclined square cavity for a laminar natural convection. They showed that the thermal boundary layer is considerably affected by the wavy wall and that the mean nusselt number decreases compared with the heat transfer in the square cavity. They

recommended investigating the hot wall geometry optimisation.

In the present study, a numerical investigation of the influence of the hot wall geometry on a laminar natural convection in an inclined square cavity, differentially heated, has been performed.

**Analysis:** The problem treated is a two-dimensional heat transfer in an inclined square cavity. The hot wall is wavy with a constant temperature  $T_h$ . The cold wall is opposite to the latter with a constant temperature  $T_c$  while the other sides are insulated. The rayleigh number is varied up to  $10^6$  while prandtl number is fixed to be 0.71. Figure 1 shows the geometrical features of the cavity used.

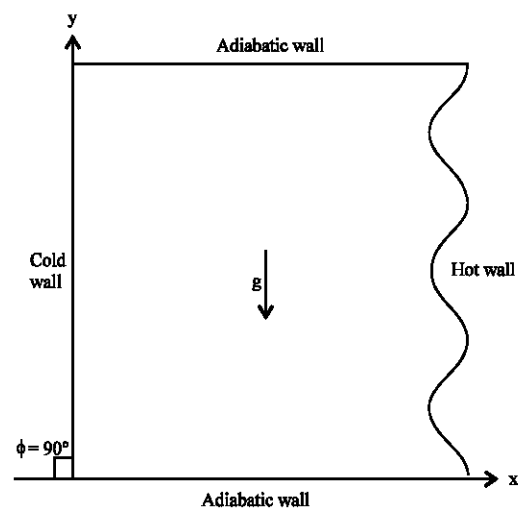


Fig. 1: Geometrical features of the undulated cavity

The viscous incompressible flow inside a closed cavity and a temperature distribution is described by the Navier-stokes and the energy equations. The boussinesq approximation is used with the assumptions of constant properties and negligible viscous dissipation. The governing equations are defined as follows:

$$\frac{\partial^2 \Psi}{\partial x^2} + \frac{\partial^2 \Psi}{\partial y^2} = -\omega \quad (1)$$

$$\frac{\partial \omega}{\partial t} + u \frac{\partial \omega}{\partial x} + v \frac{\partial \omega}{\partial y} = \mu \left( \frac{\partial^2 \omega}{\partial x^2} + \frac{\partial^2 \omega}{\partial y^2} \right) + \rho g \beta \left( \sin \phi \frac{\partial T}{\partial y} + \cos \phi \frac{\partial T}{\partial x} \right) \quad (2)$$

$$\frac{\partial T}{\partial t} + u \frac{\partial T}{\partial x} + v \frac{\partial T}{\partial y} = a \left( \frac{\partial^2 T}{\partial x^2} + \frac{\partial^2 T}{\partial y^2} \right) \quad (3)$$

With the following boundary conditions:

$T = T_h$   $u = v = 0$  on the hot wall

$T = T_c$   $u = v = 0$  on the cold wall

$\frac{\partial T}{\partial n} = 0$   $u = v = 0$  on the remaining boundaries

$$\omega = \frac{\partial^2 \Psi}{\partial n^2} \text{ on all boundaries} \quad (4)$$

Hence, introducing the following non-dimensioned variables:

$(X, Y) = (x, y)/H$ ,

$(U, V) = (u, v)H/a$ ,

$t = at^*/H$

$\omega = \omega^* H^2/a$

$\Psi = \Psi^*/a$

$\theta = (T - T_0)/(T_h - T_c)$ , with  $T_0 = (T_h + T_c)/2$

The equations of the problem are now expressed as follows:

$$\frac{\partial^2 \Psi}{\partial X^2} + \frac{\partial^2 \Psi}{\partial Y^2} = -\omega \quad (5)$$

$$\frac{\partial \omega}{\partial t} + U \frac{\partial \omega}{\partial X} + V \frac{\partial \omega}{\partial Y} = \text{Pr} \left( \frac{\partial^2 \omega}{\partial X^2} + \frac{\partial^2 \omega}{\partial Y^2} \right) + \text{PrRa} \left( \sin \phi \frac{\partial \theta}{\partial Y} + \cos \phi \frac{\partial \theta}{\partial X} \right) \quad (6)$$

$$\frac{\partial \theta}{\partial t} + U \frac{\partial \theta}{\partial X} + V \frac{\partial \theta}{\partial Y} = \left( \frac{\partial^2 \theta}{\partial X^2} + \frac{\partial^2 \theta}{\partial Y^2} \right) \quad (7)$$

The rayleigh number and prandtl number are defined as:

$$\text{Ra} = \bar{\rho} g H^3 (T_h - T_c) / a \nu \quad \text{Pr} = \nu / a \quad (8)$$

The system is completed with the following boundary conditions:

$$U = V = 0; \quad \omega = \frac{\partial^2 \Psi}{\partial n^2} \text{ on all boundaries} \quad (9)$$

$$\theta = -\frac{1}{2} \text{ on the cold wall} \quad (10)$$

$$\theta = \frac{1}{2} \text{ on the hot wall} \quad (11)$$

**Numerical method:** The grid generation calculation is based on the curvilinear co-ordinate system applied to fluid flow as described by Thompson *et al.*<sup>[12]</sup>. The transformation is as follows:

$$\epsilon = \epsilon(x, y) \text{ and } \eta = \eta(x, y) \quad (12)$$

for:

$$0 \leq \epsilon \leq 1 \text{ and } 0 \leq \eta \leq 1$$

Knowing that :

$$0 \leq y \leq 1 \text{ and } 0 \leq x \leq f(y)$$

with:

$$f(y) = [1 - \text{Amp} + \text{Amp} (\cos 2\pi n y)]$$

$$\eta = y \text{ and } x = x(\epsilon, \eta) \quad (13)$$

The heat transfer rate by convection in an enclosure is obtained from the nusselt number calculation. On the wavy wall, the local nusselt number is expressed as:

$$\text{Nu}_l = \frac{d\theta}{dn} \quad (14)$$

While, the mean nusselt number is the average of the local nusselt number along the wavy wall and is defined by the following equation:

$$\text{Nu}_a = \frac{1}{s} \int_0^s \frac{d\theta}{dn} ds \quad (15)$$

The governing equations have been transformed in calculation domain<sup>[11]</sup>. These equations are discretised by a finite difference method. The resolution of the equation system is performed by an implicit method with an alternating direction implicit scheme.

## RESULTS

Several grids have been tested for the case of  $\text{Ra} = 10^6$  and  $\phi = 90^\circ$  on the square cavity compared with

Table 1: Comparison of nusselt number at several grids for square cavity and  $Ra = 10^5$

Grid	40x40	50x50	60x60	De Vahl Davis <sup>[3]</sup>
$Nu_a$	8.927	8.837	8.773	8.80

Table 2: Mean nusselt number for  $Ra = 10^5$  and  $Ra = 10^6$

Ra	$10^5$	$10^6$	$10^5$ (%)	$10^6$ (%)
$Nu_a$ for 4 und.	3.400	6.817	23.0	22.8
Length for 4 und.	1.260	1.260	26.0	26.0
$Nu_a$ for 5 und.	3.079	6.039	30.4	31.7
Length for 5 und.	1.337	1.337	33.7	33.7
$Nu_a$ for 6 und.	3.067	5.492	30.7	37.8
Length for 6 und.	1.395	1.395	39.5	39.5

De Vahl Davis results<sup>[3]</sup>. Table 1 shows the average nusselt number for the three grids used, at  $Ra = 10^5$   $\phi = 90^\circ$ .

It is clearly seen that there is a little difference between the three grid results and the grid of (50x50) is used in all subsequent calculations. For all the tests investigated, the amplitude of the undulation was 0.05.

The discussion of the presented results concerns, the streamlines and the temperature distributions, the local nusselt number and the heat transfer rate for the three configurations at different inclination angles ( $\phi = 0^\circ$ ,  $\phi = 45^\circ$ ,  $\phi = 90^\circ$ ,  $\phi = 120^\circ$ ,  $\phi = 150^\circ$  and  $\phi = 180^\circ$ ). For all the configurations, the flow structure is similar to that found for the square cavity<sup>[13]</sup>.

**Temperature and streamline distributions:** Figure 2-7 show respectively, the streamlines and the temperature distributions for the configurations tested. At  $\phi = 45^\circ$  it can clearly be seen that near the wavy wall, the thermal boundary layer thickness increases in the flow direction resulting in a decrease in the local heat transfer along this wall. This is due to the undulation of the wall. However, the heat transfer by diffusion remains dominant in the core region.

At the angle of  $\phi = 90^\circ$ , the gravitation is perpendicular to the adiabatic walls. Figure 3, 5 and 7 show the thermo convective flow accelerating more and is represented by the form of one diagonally stretched cell.

The thermal boundary layer thickness for  $\phi = 90^\circ$  is slightly higher than for the two other angles on the second half of the hot wall. The latter is confirmed by the increase in local nusselt number for this angle.

**Local heat transfer:** Figure 8-10 represent a comparison between the local nusselt number distributions for the three configurations tested for an inclination angle of  $90^\circ$  and  $Ra = 10^5$ . It is clearly seen that the local nusselt number has a sinusoidal trend for all tested cavities. The lowest local heat transfer is for the configuration with six

undulations. The number of the peaks in the local nusselt number curves corresponds to the undulation number of the hot wall. This remark is valid for all the performed angles. It appears that the difference between the different local nusselt numbers vanishes after the first peak for an angle equal or more than  $90^\circ$ . For an angle of  $0^\circ$ , the average local heat transfer seems to have a value of about one corresponding to the conduction regime.

**Global heat transfer with angle:** Figure 11 shows the averaged nusselt number with the variation in the inclination angle for rayleigh number of  $10^5$ . For the square cavity, the curve used here, is obtained by the formulae of Zhong *et al.*<sup>[8]</sup> expressed as follows:

$$Nu_a = (Nu_a(90^\circ) - Nu_a(0^\circ)) \times (2/\pi) \times (\phi \sin(\phi)) + Nu_a(0^\circ) \text{ for } \phi \leq 150^\circ \quad (16)$$

$$Nu_a = Nu_a(180^\circ) \times (\cos(\phi - 180^\circ)) \text{ for } \phi > 150^\circ$$

It is clearly seen that all configurations have the same trend. The maximum heat transfer occurs for an angle between  $100^\circ$  and  $130^\circ$  for the configurations with 4 and 5 undulations. However, for the configuration with six undulations, this maximum is shifted to an angle of  $150^\circ$ . There is a little difference in the local nusselt number in the range of  $0$ - $120^\circ$ .

For all the configurations tested, the averaged nusselt number remains low in the range of  $0$ - $180^\circ$ . It can also be noted that the average nusselt number decreases about an angle of  $180^\circ$ . This result is in agreement with the Ozoe *et al.*<sup>[14]</sup>.

**Global heat transfer function of rayleigh number:** Figure 12 shows the comparison of the average nusselt number function of rayleigh number for all the configurations and for the square cavity at an angle of inclination of  $90^\circ$ . The comparison is for a Rayleigh number up to  $10^6$ . The influence of the hot wall geometry is well established by a clear decrease in the global heat transfer compared with the square cavity. It is clearly seen that the difference between the averaged nusselt number of the square cavity, cavity with three undulations<sup>[11]</sup> and the tested configurations increases with an increase in the rayleigh number.

The relative decrease of the mean nusselt number, respectively for the cavity with four, five and six undulations is (23, 30.4 and 30.7%) for  $Ra = 10^5$  and (22.8, 31.7 and 37.8%) for  $Ra = 10^6$  compared with the

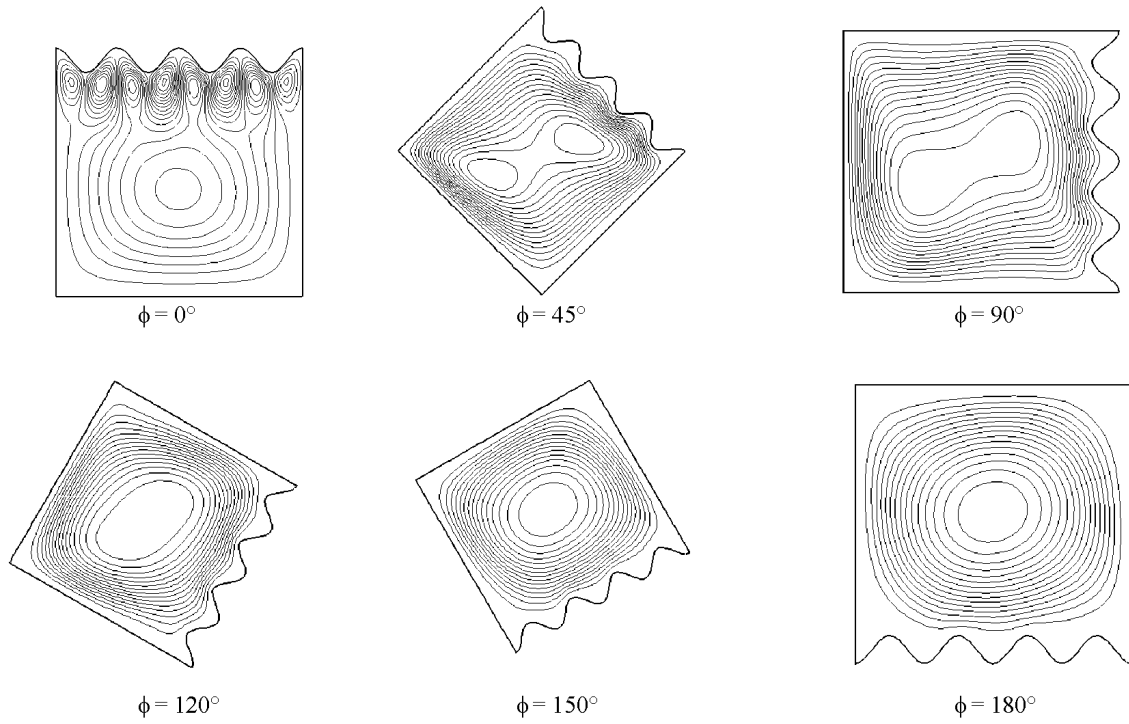


Fig. 2: Streamlines for different inclination angles for a cavity with four undulations

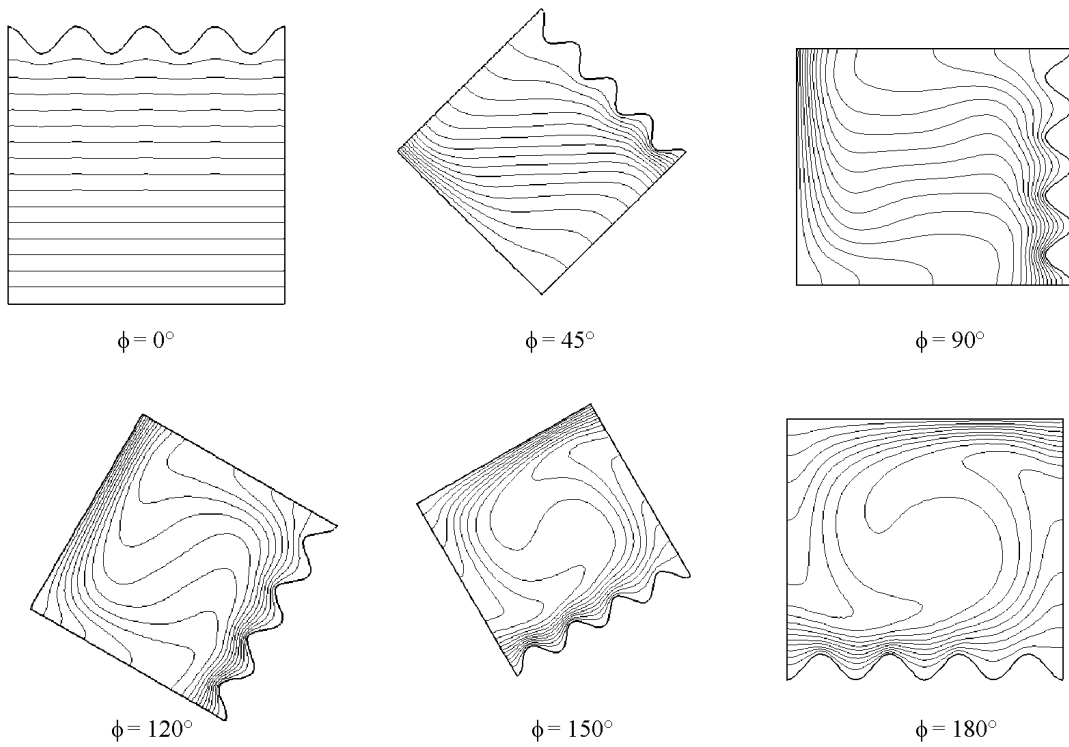


Fig. 3: Isotherms for different inclination angles for a cavity with four undulations

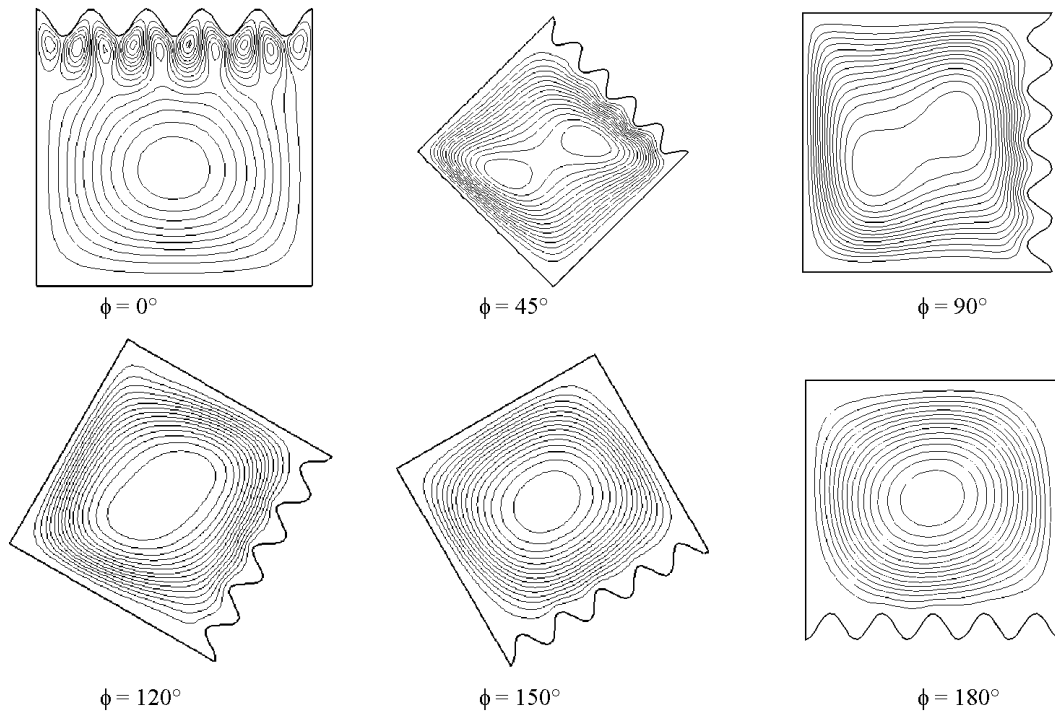


Fig. 4: Streamlines for different inclination angles for a cavity with five undulations

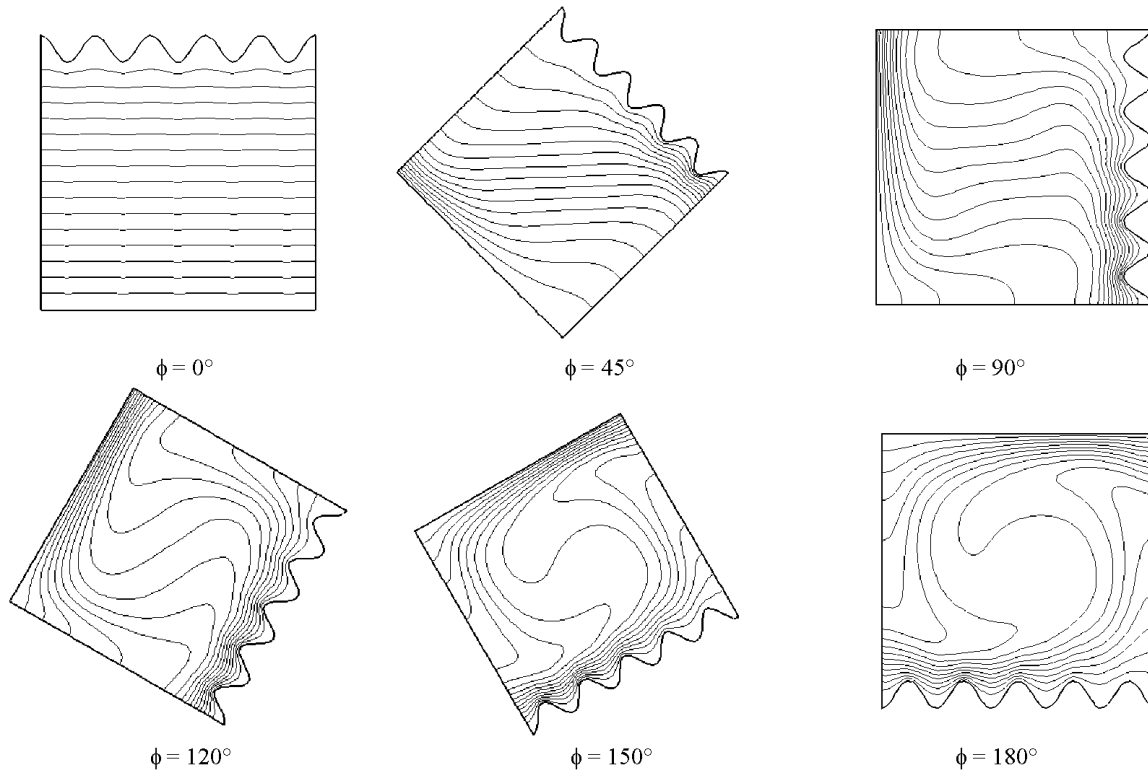


Fig. 5: Isotherms for different inclination angles for a cavity with five undulations

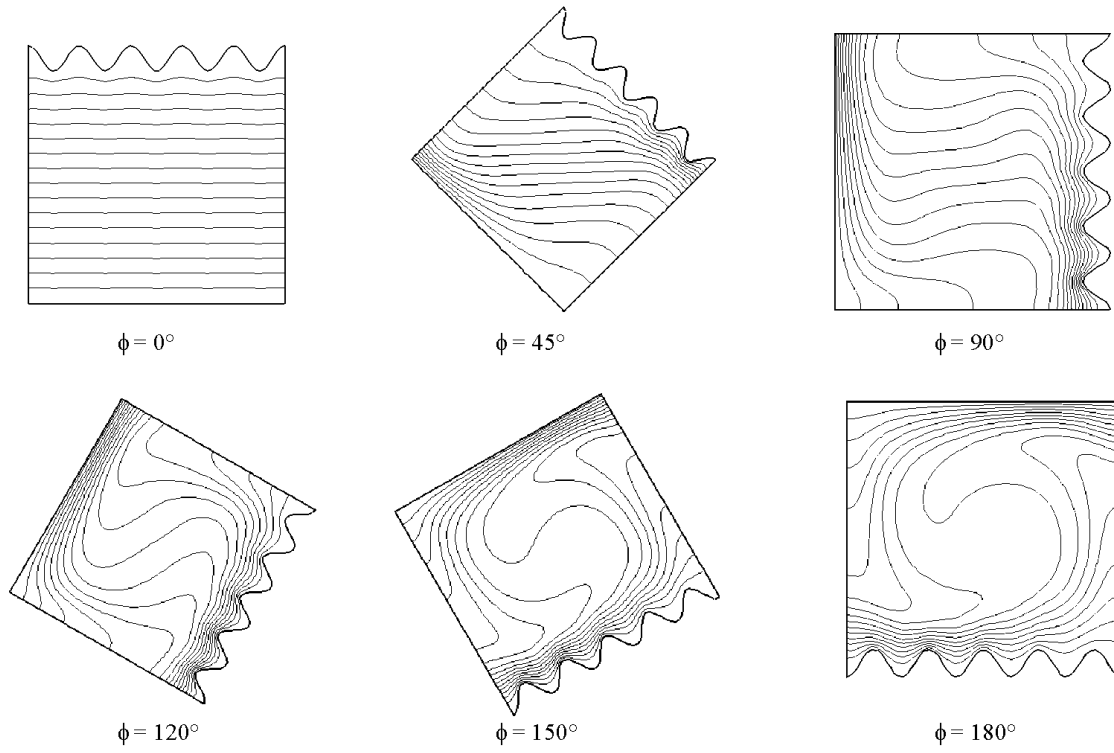


Fig. 6: Streamlines for different inclination angles for a cavity with six undulations

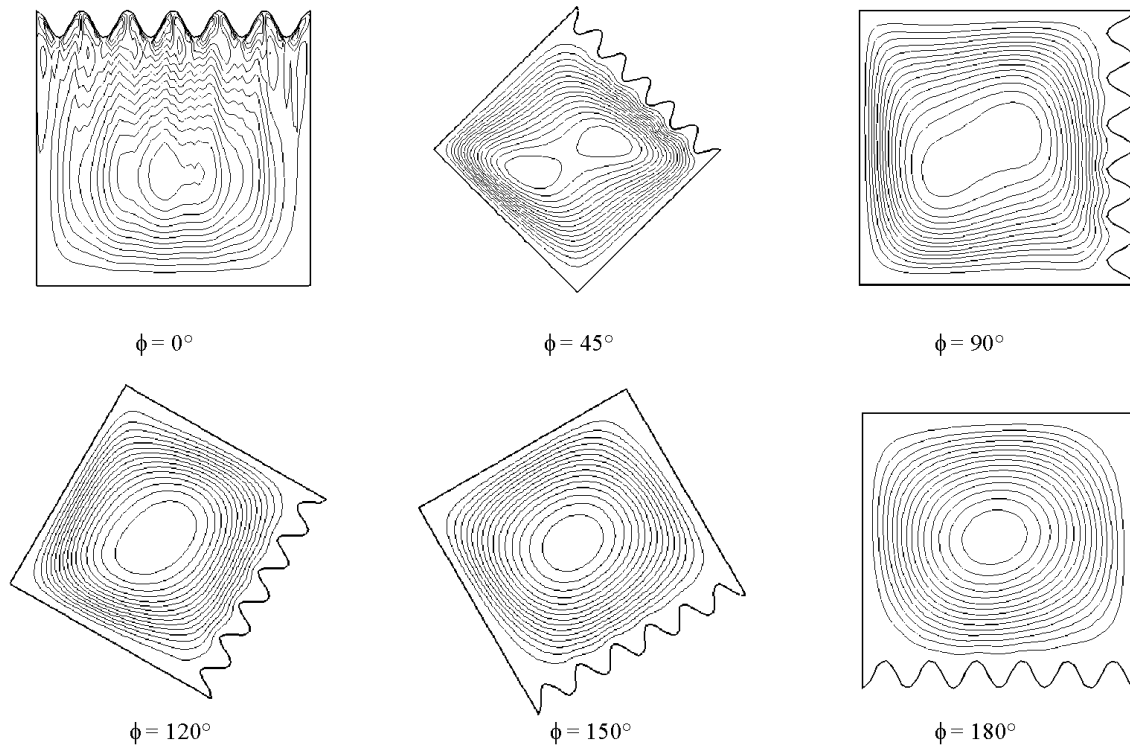


Fig. 7: Isotherms for different inclination angles for a cavity with six undulations

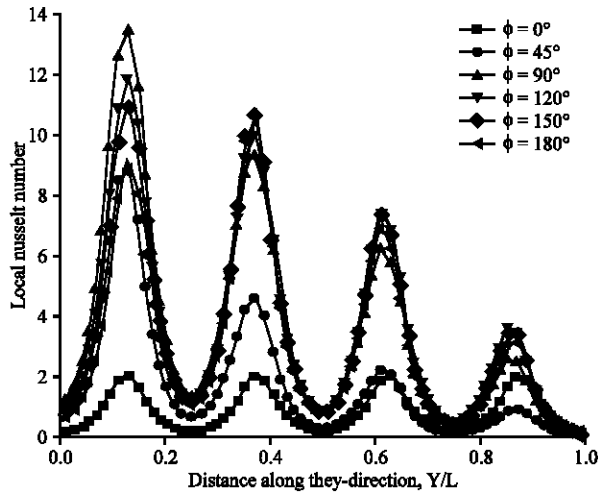


Fig. 8: Local nusselt number distributions for a cavity with four undulations

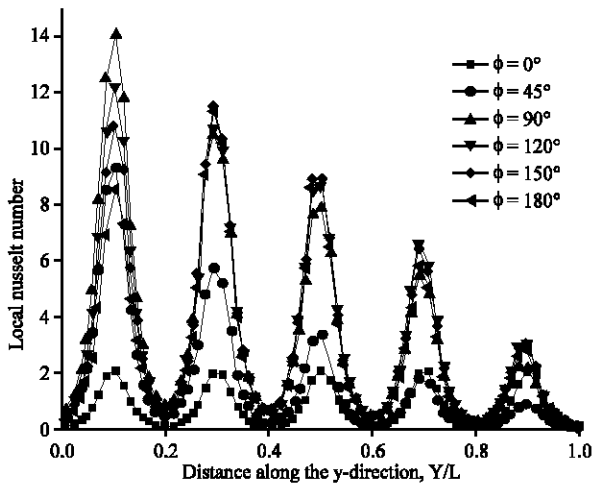


Fig. 9: Local nusselt number distributions for a cavity with five undulations

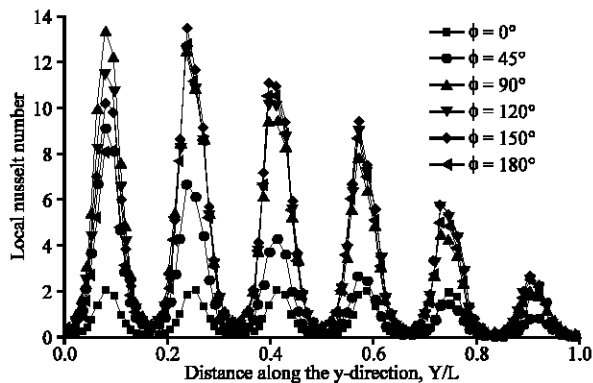


Fig. 10: Local nusselt number distributions for a cavity with six undulations.

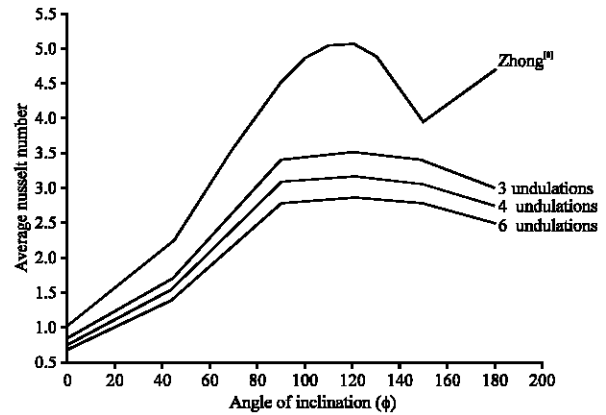


Fig. 11: Comparison of the mean nusselt number at  $Ra = 10^5$

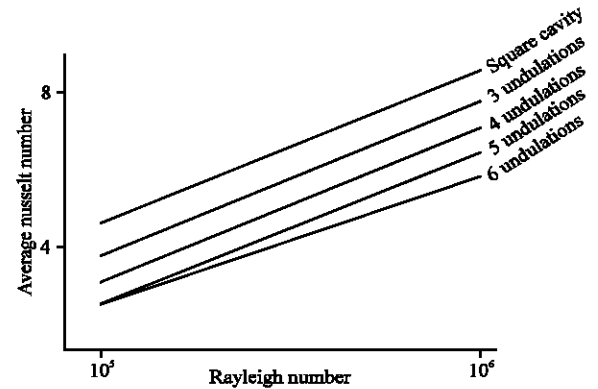


Fig. 12: Comparison of the mean nusselt number for  $\phi = 90^\circ$

averaged heat transfer in the square cavity. On the other hand, the increase of the heat exchange area is respectively (26, 33.7 and 39.5%) for four, five and six undulations. The heat transfer by convection decreases slightly (Table 2). Furthermore, in a solar collector for example, the exchange by radiation increases with the increase of the exchange area.

## CONCLUSIONS

The effect of the hot wall geometry in an inclined square cavity on the heat transfer by natural convection is investigated in the present study.

The results obtained for different rayleigh numbers and for different inclination angles show that the flow and the heat transfer are affected by the change in the hot wall geometry. The mean nusselt number decreases compared with the global heat transfer in the square cavity. It reaches respectively 30.7 and 37.8% at  $Ra = 10^5$  and  $Ra = 10^6$  for the configuration with six undulations.



# **Nomenclature:**

a	thermal diffusivity;
g	gravitational acceleration;
l	width of the cavity;
n	normal to the wall;
Nu	Nusselt number;
Pr = $\nu/\alpha$	Prandtl number;
	$Ra = \frac{\beta g l^3 (T_h - T_c)}{(\alpha \nu)}$
	Rayleigh number;
s	curvilinear coordinate on the wavy wall;
T	temperature;
u,v	velocity components on x and y;
x,y	cartesian co-ordinates.

## Greek symbols

$\beta$	thermal dilatation coefficient;
$\epsilon, \eta$	co-ordinates of the transformed domain;
$\nu$	kinematic viscosity;
$\rho$	density;
$\phi$	inclination angle;
$\Psi$	stream function;
$\omega$	vorticity;

$\frac{\partial}{\partial n}$	normal gradient.
-------------------------------	------------------

## Indices

a	average;
l	local;
h, c	hot wall and cold wall
x,y,t	derivative relative to x,y and t.

## ACKNOWLEDGMENTS

The authors wish to give special thanks for Prof. A Taleb-bendiab of John Moore University Liverpool, Prof. Marcillat IMF de Marseille.

## REFERENCES

1. Jones, J.P., 1979. A Comparison Problem for Numerical Method in Fluid Dynamics: The Double Glazing Problem. Numerical Methods in Thermal Problem, Pineridge Press, Swansea, UK., pp: 338-348.
2. Mallinson, G.D. and G. De Vahl Davis, 1973. The method for the false transient for the solution of coupled partial differential equation. J. Comput. Phys., 12: 435-445.
3. De Vahl Davis, G., 1983. Natural convection of air in a square cavity: A benchmark numerical solution. Intl. J. Numerical Methods Fluids, 3: 249-264.
4. Saitoh, T. and K. Hirose, 1989. High accuracy benchmark solution to natural convection in a square cavity. Computational Mechanics, pp: 417-427.
5. Hassan, M.N.W., 1994. A numerical solution of fluid and heat flow in a triangular enclosure. Intl. Conf. Fluid Thermal Energy Conversion, Bali, Indonesia, pp: 315-320.
6. Lin, F.N. and B.T. Chao, 1974. Laminar free convection over two dimensional and axi-symmetric bodies of arbitrary contour. J. Heat Transfer, 96: 163-170.
7. Raithby, G.D. and K.G.T. Hollands, 1995. Laminar and turbulent free convection. Adv. In: Heat Transfer, Academic Press, New York, 11: 72-80.
8. Zhong, Z.Y., K.T. Yang and J.R. Lloyd, 1985. Variable Property Natural Convection in Tilted Cavities with Thermal Radiations. In: Lewis, R.W. and V.T. Morgan (Eds.), Numerical Methods in Heat Transfer, 3: 195-214.
9. Arnold, J.N, I. Catton and D.K. Edwards, 1976. Experimental investigation of natural convection in inclined rectangular regions of different aspect ratios. J. Heat Transfer, 95: 67-71.
10. Yao, L.S., 1983. Natural convection along a vertical wavy surface. J. Heat Transfer, 105: 465-468.
11. Adjilout, L., O. Imine, A. Azzi and M. Belkadi, 2002. Natural convection in an inclined cavity with a wavy wall. Intl. J. Heat Mass Transfer, 45: 2141-2152.
12. Thomson, P.D., F.C. Thames and F. Mastin, 1974. Automatic numerical generation of body-fitted curvilinear co-ordinate system. J. Comput. Phys., 15: 299-319.
13. Hammady, F.J., J.R. Lloyd, H.Q. Yang and K.T. Yang, 1989. Study of local natural convection heat transfer in an inclined enclosure. Intl. J. Heat Mass Transfer, 32: 1697-1708.
14. Ozoe, H., K. Fujii, N. Lior and S.W. Churchill, 1983. Long rolls generated by natural convection in an inclined rectangular enclosure. Intl. J. Heat Mass Transfer, 26: 1427-1438.